Experimental Studies of the Effect of Ethanol Auxiliary Fuelled in Turbulent Jet Igniter in an Optical Engine

Bureshaid K, Shimura R, Feng D, Zhao H and Bunce M

Abstract:

Due to emission legislations, searching for alternative and sustainable energy sources to improve air quality and reduce emissions. It is believed that ethanol can replace fossil. Ethanol can be used in spark-ignition (SI) engines as a pure or blended fuel. Ethanol has 2.6 times higher latent heat of vaporization (HOV) than conventional gasoline per unit of mass and 4.2 times higher latent heat of vaporization for a stoichiometric mixture. Thus leads to reduce the charge temperature and exhaust emissions such as NOx. Ethanol shows faster combustion compared to gasoline due to higher laminar flame speed, and extending MBT operation range.

Turbulent Jet Ignition (TJI) is an advanced ignition system that replaced standard spark ignition in combustion engines. Turbulent Jet Ignition offers very fast burn rates compared to spark plug ignition due to the ignition system producing multiple ignition sites that consume the main charge rapidly. The pre-chamber combustion produces high energy ignition system to ignite the main chamber mixture. Therefore, TJI allows for increased levels of dilution. However, previous experimental studies highlighted the effect of gasoline fuel in pre-chamber ignition but this work investigates optically the effect of ethanol as well as gasoline fuel in the combustion process in a single cylinder optical engine. Additionally, this paper focuses on the effect of injection fuel, spark timing and injection timing in jet formation for both fuels. The results show that increasing the fuel injected in the pre-chamber, the pre-chamber pressure rises faster to a higher peak value and produces greater pressure differential between the pre and main chamber. Increasing pre-chamber pressure causes the jets to travel deeper into the main chamber and the ignition sites become bigger. The injection timing has less effect on combustion stability. However, as the injection timing and spark timing were advanced, the combustion became unstable. Ethanol shows more combustion stability compared to gasoline. This is because ethanol had the fastest flame speed and appeared to exhibit less cyclic variation.

1. Introduction:

Increasing concerns on the environmental issues due to engines emissions have led most nations to propose even more constraints for both engines and fuels. In order to ease environmental stress, particularly cutting greenhouse emissions, and confront the rising energy demand, it should to search for alternative and sustainable energy sources to improve the fuel supply chain. Great efforts are dedicated to improve the combustion process to reduce the fuel consumption and exhaust emissions. It is believed that biofuels can offer a viable short- to mid-term solution [1]. Among many biofuels, ethanol is currently most promising alternative fuel for internal combustion engines [2]. It offers many advantages over other fossil fuels due to the lower combustion temperature resulting in reduced NOx emissions. Moreover, ethanol has higher RON and MON than gasoline which increase the knock resistance at higher loads and improves combustion phasing. Additionally, ethanol has

2.6 times higher latent heat of vaporization (HOV) than conventional gasoline per unit of mass and 4.2 times higher latent heat of vaporization for a stoichiometric mixture [3]. This reduces the charge temperature and may increase volumetric efficiency. For example, In the United States, addition of ethanol in gasoline has been promoted by tax incentives to try to replicate the biofuel success in Brazil [4, 5].

However, the major challenges facing spark ignition engines are the slow flame propagation speed and unstable combustion under lean condition which affects to decrease the engine power output and increase the fuel consumption [6]. To overcome all these negatives, the ignition was enhanced to increase the ignition energy by using pre-chamber ignition system. Pre-chamber is the most successful technology that can be used to burn lean/ ultra-lean mixture. The pre-chamber design and concept have been developed for several years [7, 8, 9, 10, 11, 12]. The jet ignition system works to inject a chemical radicals with high turbulent jet to initiate lean fuel mixtures in the main chamber. Then, these radicals travel to the main chamber through an orifice or orifices, igniting the main chamber air-fuel charge. With jet ignition, pre-chamber is able to ignite the main chamber with further lean $\lambda > 1.4$.

The pre-chamber technology was discovered in the beginning the twentieth of century with two stroke Ricardo Dolphin engines by Harry. He implemented an extra intake valve to increase the inlet air [13]. Another significant aspect of lean combustion is the torch cell engine where this idea was developed from an axillary valve. In torch cell engine needed to have an auxiliary pre-chamber fuelling system. The pre-chamber contains a spark plug and is filled with air during compression stroke [14]. Jet igniter is a part of the divided chamber stratified charge concept. Jet igniters contain much smaller orifice(s) connecting the main chamber and pre-chamber combustion cavities. The smaller orifice/ orifices creates a flame jet that penetrates deeper into the main charge. As mention before, pre-chamber injects high reactive radicals where jet ignition chemical kinetics control the combustion characteristics. In 1950s, the jet ignition system was presented by Nikolai [12]. Then, this idea was evolved by Gussak where he used small pre-chamber size [15]. Table 1 summarize the development in jet ignition system with a small pre-chamber.

Table 1. Literature review of jet ignition studies with small pre-chamber volumes (< 3% clearance volume).

Date	Jet Ignition System	Done by
End 1970	Jet Plume Injection and Combustion (JPIC)	Oppenheim et al. [16].
1984	Swirl Chamber Spark Plug	Reinhard Latsh [17].
1992	Hydrogen Assisted Jet Ignition (HAJI)	H.C. Watson et al. [18].
1993	Pulsed Jet Combustion	Warsaw [19].
1993	Hydrogen Flame Jet Ignition (HFJI)	Toyota College [20].
1999	Self-Ignition Triggered by Radical Injection (APIR)	University of Orleans [21].
1999	BPI- Bowl Pre-Chamber Ignition	University of karlsruche and Multitorch [22]
2003	Pulse Jet Igniter (PJI)	Najt et al. [23]

2005	Homogenous Combustion jet Ignition (HCJI).	Robert Bosch. [24]
2007	IAV Pre-Chamber Spark Plug with Pilot Injection.	IAV GmbH and Multitorch [25].
2009	Turbulent Jet Ignition (TJI).	Mahle Powertrain [7].

The current work aims at deepening the knowledge of the effects the ignition enhancement in combustion process by comparing normal spark plug (SI) with turbulent jet ignition (TJI). Also, the effect of ethanol will be evaluated in both ignition system under different air-fuel ratios. Differences in engine performance, heat release and combustion and flame propagation are compared and benchmarked with results of conventional gasoline, by simultaneous in-cylinder pressure measurements and high-speed flame chemiluminescence imaging. However, the previous studies were focused on turbulent jet ignition system that fuelled by gasoline with thermodynamic and imaging analysis. In this work the possibility of alternative fuels was evaluated based on criteria for example lean limit and effects on combustion parameters with deep study by using ICCD imaging technique to gain further understanding of the pre-chamber combustion event and jet formation. This is because the jet ignition system is different from normal spark combustion as will be explained later.

During this project, pre-chamber that utilizes Mahle Jet Ignition (MJI) which was patented by MAHLE Powertrain, was used. The pre-chamber volume is very small relative to previous pre-chamber to reduce heat loss. Further, a small pre-chamber surface emits fewer hydrocarbon (HC) emissions due to the reduced crevice volume and combustion surface area. The pre-chamber is connecting to the main chamber by 6 orifices. The pre-chamber concept based on [9] have the following aspects;

- Small pre-chamber volume (< 5% of main chamber volume at TDC).
- Multiple-orifices nozzle connecting pre-chamber to main chamber.
- Small orifice diameter to promote flame quenching.
- Separate fuelling strategies for pre-chamber and main chamber.

Figure 1 and 2 display computer design images of the pre-chamber installed in the optical engine. By using small orifice diameter, it helps to quench the injected flame from pre-chamber to main chamber. In addition, the quenching flame enters the main chamber with high turbulent that allows to goes deeper into the main charge and to fully burn main chamber charge. Also, turbulence ensures the interaction between radicals and main chamber charge. Both chambers fuelled with two separate fuel systems, main chamber was fired with PFI injector, while the pre-chamber was fuelled by DI injector. The benefit of the fuelling pre-chamber with DI injector is to allow precise and de-coupled control over the mixture in both chambers. Multi-orifices gives more charge distribution in the main chamber. Thus, pre-chamber produces full combustion. Further review of pre-chamber design has been documented [26, 27, 28].

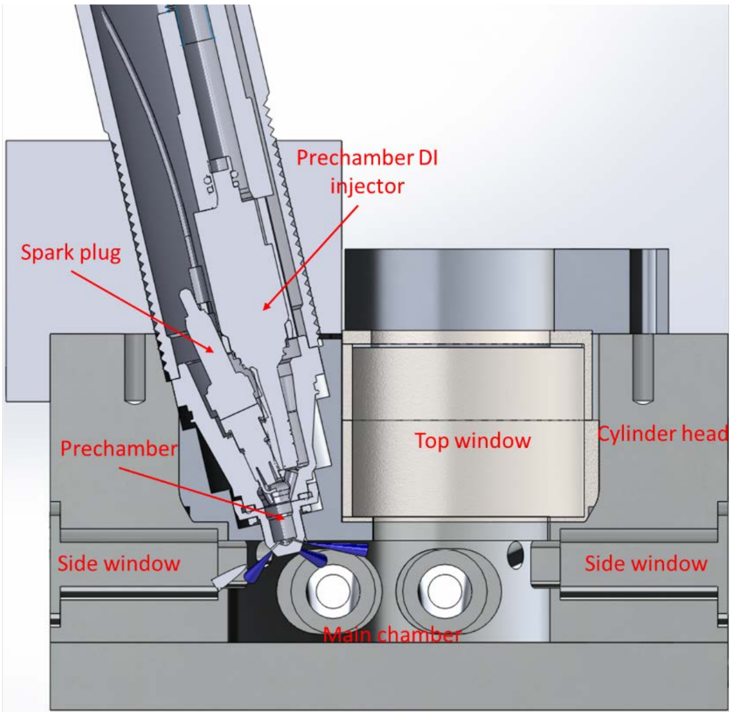

Figure 1. Sectioned view of the MJI unit installed in the optical engine

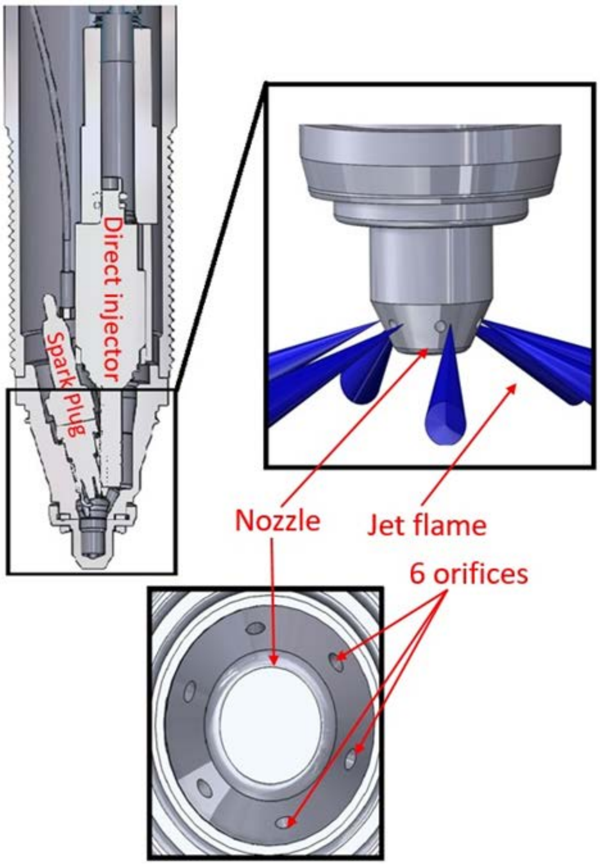

Figure 2. Design ismage shows the MJI pre-chamber and nozzle inside.

2. Experimental Setup:

In this study a customized single cylinder optical engine was used with its cylinder head modified for the MTJ installation. The bottom-end of the engine is based on a commercial Lister Petter TS1 with a modified flat piston crown. Both intake and exhaust valves are located on the sides so that a full view of the combustion chamber can be realised by the installation of an optical window at the top. As shown in Figure 3, in order to fit the MJI unit, the cylinder head was modified by splitting the top of the cylinder head into two parts. The MTJ unit was installed in one side and a half circular window on the other side for the optical access from the top. Two optical windows flushes mounted at the top of the cylinder block can be used to gain the optical access from the side. The quartz windows are designed to withstand peak in-cylinder pressures up to 150 bar.

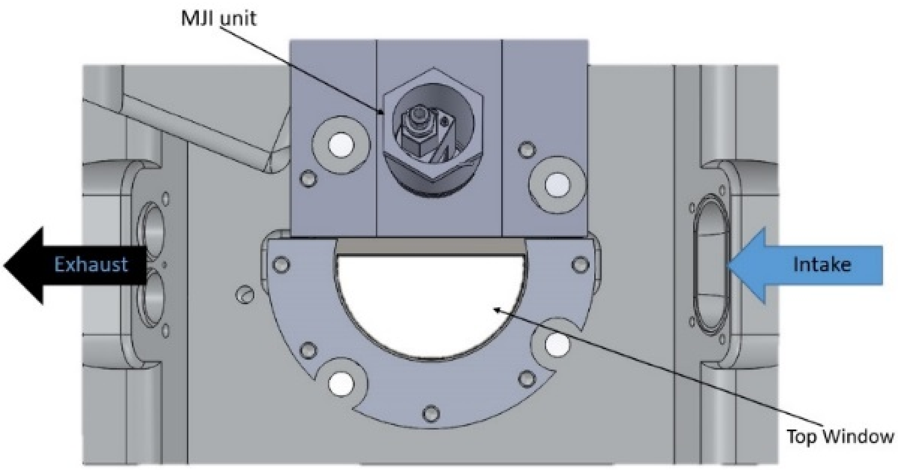

Figure 3. Schematic view of cylinder head

The basic geometry of the engine is provided in Table 2. The engine has one inlet and two exhaust valves. To maintain realistic valve durations and overlap, the side mounted poppet valves are recessed into special cylindrical pockets within the chamber side walls.

Table 2. Basic engine geometry

Parameter	Value (unit)
Displacement	631 cc
Cylinder	1
Bore	95 mm
Stroke	89 mm
Compression Ratio	8.4:1
Exhaust valve	140/370 (°aTDC)
Valve overlap	25 (CA)
Inlet valve opening/closing	345/575 (°aTDC)

Valve lift	5 mm

The ignition system in the main chamber comprises of an NGK ER9EH 8mm spark plug and a Bosch P100T ignition coil. The engine is coupled to a 10kW DC motor dynamometer via a flexible coupling. The fuel in the main chamber is supplied from a 5.0 litre fuel tank at 3 bar gauge pressure and injected into the intake port by a Bosch EV6 Port fuel injector installed in front of the intake valve. A filter was fitted between the fuel tank and the pump to remove the majority of particles from fuel. The in-cylinder and pre-chamber pressure weres measured by an AVL piezoelectric pressure transducer (GH14DK) and charge amplifier and its output was recorded and digitised by a high-speed USB type LabVIEW data-logging card (DAQ) at four samples per crank angle degree via a digital shaft encoder that connected to the intake camshaft. To determine the overall air/fuel ratio, a Bosch LSU 4.2 UEGO sensor (Universal Exhaust Gas Oxygen sensor) was fitted to the exhaust pipe. The UEGO sensor was connected to an ETAS LA4 lambda meter. The intake plenum absolute pressure was recorded by a Gems 1200 series CVD sensor. The intake and exhaust temperatures were measured by k-type thermocouples which were fitted downstream of the inlet air heater and in the exhaust ports, respectively. The heat release analysis was performed using an in-house MATLAB program on the averaged cylinder pressure over 300 cycles, recorded in discrete 100 cycle batches. The ignition system for MJI uses the same NGK ER9EH 8mm spark plug and Bosch P100T ignition coil. Fuel injection into the pre-chamber is achieved by a small DI injector at 70 bar from a high pressure air driven diaphragm pump.

3. Optical measurement

High-speed imaging was used to study the ignition and combustion processes in the cylinder between the main chamber spark ignition and pre-chamber ignition. To obtain the ignition and combustion image, an endoscopic probe was used, as shown in Figure 4. The sapphire window was fixed in place via an adapter and sealed with gasket to prevent the gas leakage. The ICCD camera had an array size of 1024 x 1024 pixels with a pixel size of 13 x 13 μm and 16-bit dynamic range at a digitization rate of 10 MHz (figure 5). On the other hand, the high speed camera was used to capture the combustion and that also gives the opportunity to study the combustion process. The frame rate was set at 4500 fps with resolution 1024 x 992. The synchronization of the ICCD and high speed camera with the engine was driven by the trigger signal at a given crank angle through a delay generator. The intensifier-gate delay was set at 31 ns, and width of 0.81 μs at 1200 rpm for imaging technique in order to have a good accuracy.

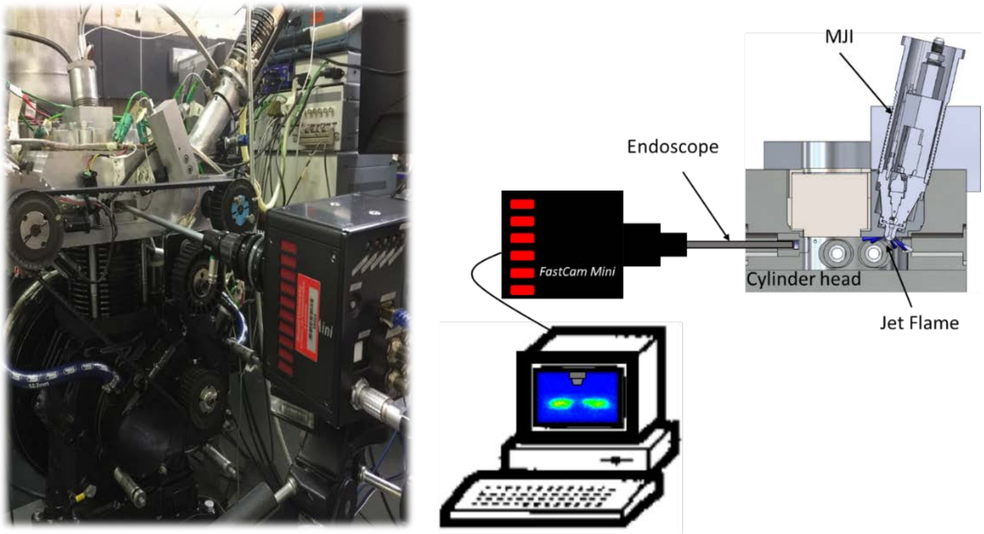

Figure 4. Picture and schematic of high speed imaging setup

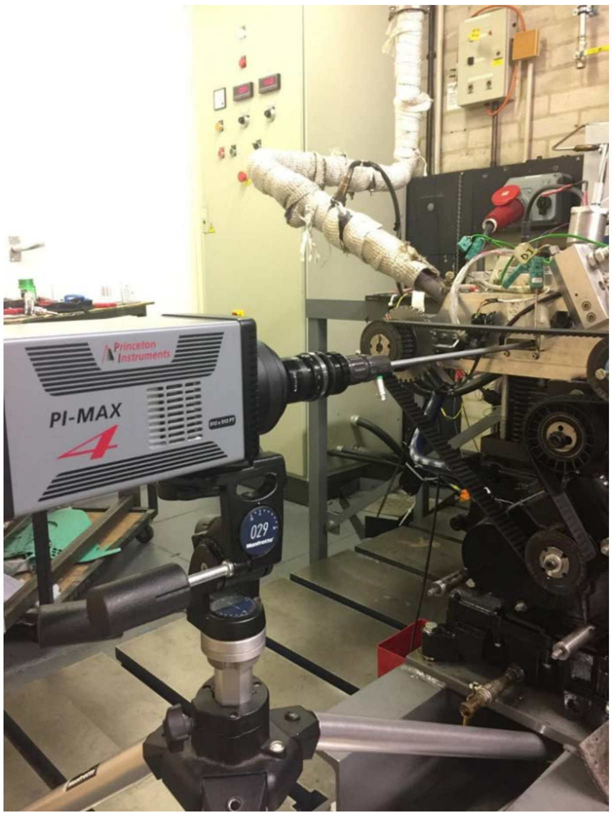

Figure 5. Picture of ICCD imaging setup

4. EXPERIMENTAL TEST CONDITIONS

All experiments were carried out at 1200 rpm and wide-open-throttle (WOT) with gasoline or ethanol. The spark timing was fixed at 22 °CA bTDC for the main chamber ignition and 10 °CA bTDC for the pre-chamber ignition, which produced similar pressure traces at baseline engine operation at different air/fuel ratios. To increase λ (the relative air-fuel ratio), the fuel amount was reduced while the inlet air pressure was fixed at 1 bar. The upper limit of the coefficient of variation of the IMEP (COV_{IMEP}) is defined as ≤ 5%. The fuel injection duration in the in pre-chamber was fixed at 50 ^{o}CA before the spark discharge to allow the mixture formation to take place. The pre-chamber injection fuel was set to 0.3 mg/pulse for both fuels. Based on the calculated mean gas temperature, the pre-chamber air mass was calculated and then the lambda values of pre-chamber mixture were estimated to be 0.78, and 1.09 for gasoline and ethanol, respectively. It was estimated that the thermodynamic state within the pre-chamber at the time of injection was about 5 bar and 550 K. The pre-chamber volume was 1000 mm^3 which is 1.27 % of the main chamber volume at TDC.

5. Results and Discussion

5.1 Thermodynamic results

Figure 6 shows the in-cylinder pressure traces and heat release rate for gasoline and ethanol under stoichiometric and lean condition (λ =1.1) with spark ignition in the main chamber at a fixed spark timing of 22 ^{o}CA bTDC. As shown, ethanol produces higher peak cylinder pressure at an earlier g crank angles at the same spark timing in both cases. The largest difference in maximum cylinder pressure between ethanol and gasoline occurs under stoichiometric condition, with 31.4 bar for ethanol and 29.1bar for gasoline. This is caused by the relatively faster burning rate of ethanol [29], as well as the higher energy input of ethanol in the cylinder. The lower heating values and the stoichiometric AFR of gasoline, and ethanol are 41.087 and 28.865 MJ/kg, 14.421 and 8.953, respectively. Under constant throttle (constant volumetric air flow rate) the input energy contained in a stoichiometric mixture of one kilogram of intake air and fuel are 2.92 and 3 MJ for gasoline and ethanol, respectively. As expected cylinder pressures and heat release rates drop slightly with leaner mixtures.

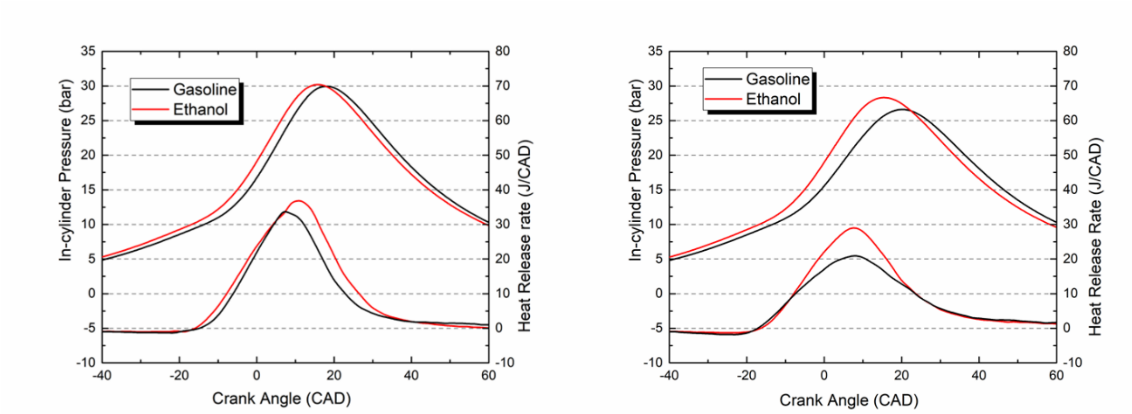

(a) λ = 1.0 (b) λ = 1.1

Figure 6. In-cylinder pressure and heat release rate curves for the main chamber spark ignition at 22 ^{0}CA bTDC

Figure 7 shows in-cylinder pressure and heat release rate with gasoline and ethanol under fixed spark timing 10 ^{o}CA bTDC in the unfuelled pre-chamber. The corresponding net IMEP of each fuel under different relative air/fuel ratios are shown in Figure 8. During the test, different air/fuel ratios were achieved by adjusting the fuel injection duration under constant throttle opening. Therefore, the highest IMEPs were obtained at lambda 1.0 with Ethanol for both ignition systems.

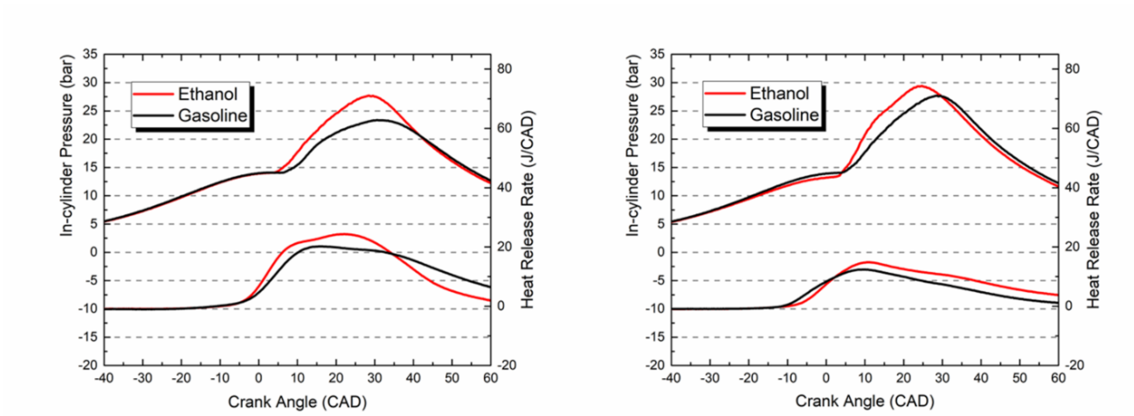

(a) λ = 1.0 (b) λ = 1.2

Figure 7. In-cylinder pressure and heat release rate at fixed spark timing 10 °CA bTDC

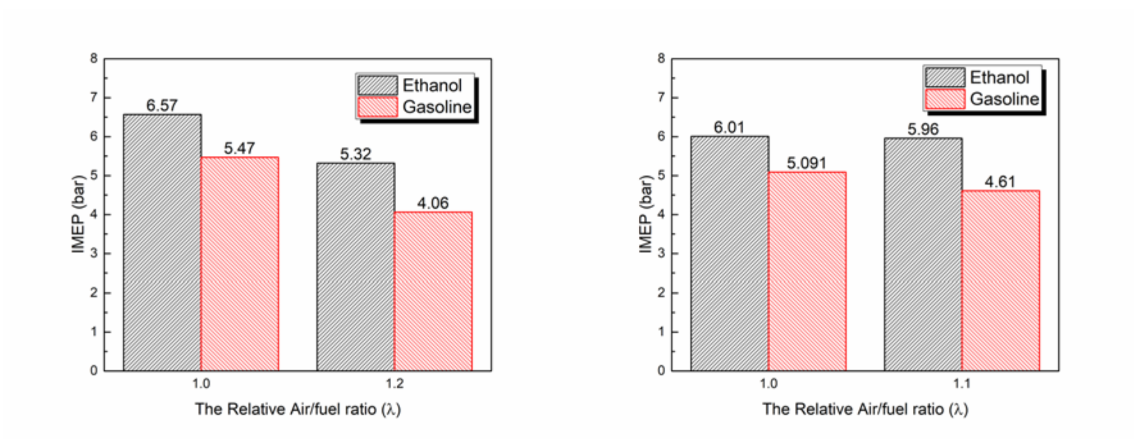

Pre-chamber ignition @ 10 °CA bTDC

Normal spark ignition @ 22 °CA bTDC

Figure 8. Effect of fuel on IMEP variation with lambda with unfuelled pre-chamber.

Figure 9 is illustrated the differences between the two ignition systems by the high-speed images of the ignition and flame propagation in the main chamber. The first visible site of combustion was located near the spark plug with ignition in the main chamber while the initial combustion appeared in more regions with greater intensity by turbulent jet ignition from the pre-chamber.

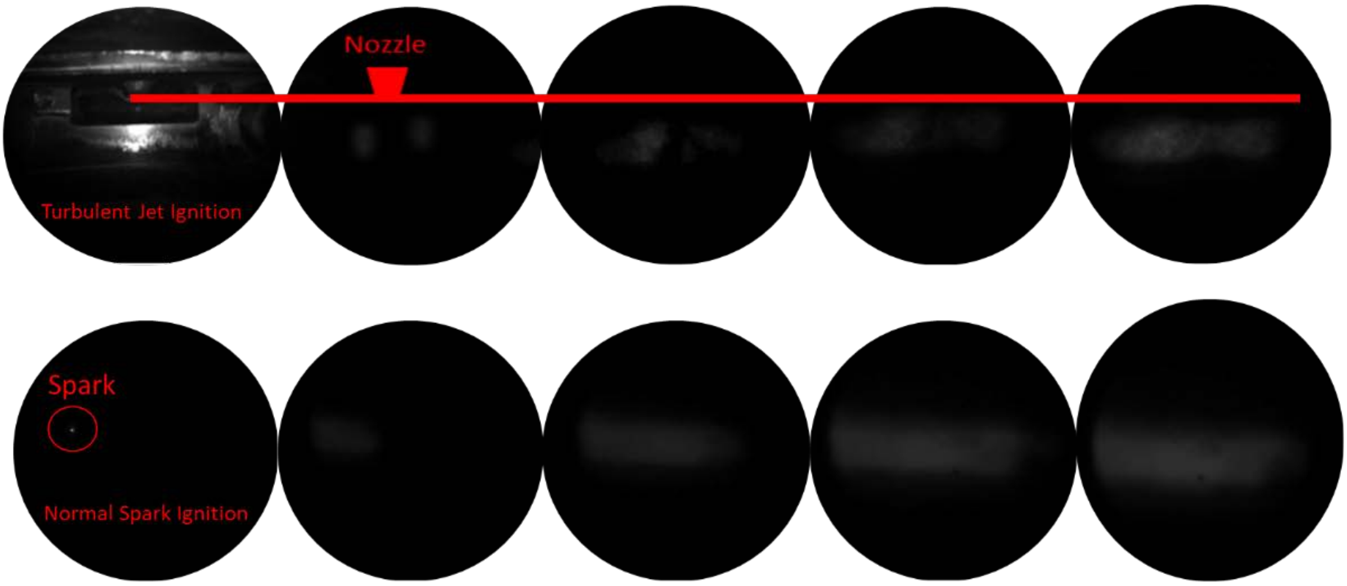

Figure 9. Shows the comparison between normal spark ignition and jet ignition system.

5.2 Optical result:

However, this report is discussed the differences between normal spark ignition and pre-chamber ignition system but this work aim to study the effect of injected radicals from pre-chamber to main chamber. In order to explain the ignition process and understand flame propagation characteristics during the combustion, an ICCD camera (*Pimax4*, Princeton) coupled with endoscope was used in place of the high speed video camera. Figure 10 and 11 show the pre-chamber and main chamber pressure and the corresponding combustion images of ethanol and gasoline at fixed spark timing of 10 °CA bTDC in the pre-chamber at lambda 1.0 and 1.2. In this case, the main chamber charge was fire with unfuelled pre-chamber. This was realized by replacing the pre-chamber injector with dummy injector. The pre-chamber is fed a pre-mixed stoichiometric/ slightly rich mixture from the main chamber due to the piston motion and subsequent flow interaction between both combustion volumes. The in-cylinder pressure traces of both the main and pre-chambers and the corresponding combustion images of lambda 1 for both fuel as shown in figure 10. Interestingly, pre-chamber pressure becomes slightly higher than main chamber pressure when spark plug at pre-chamber ignites the air/fuel mixture where it return back from main chamber to pre-chamber volume during combustion stroke. Then, the combustion continues across the pre-chamber and leads to increase the pre-chamber pressure. The ICCD camera was able to record the injected products from pre-chamber through nozzle orifices. These products were first appear at 13 °CA and 14 °CA for ethanol and gasoline, respectively. There was a delayed of the first appearance of injected products compare with fuelled pre-chamber. This is may be due to the effect of pre-chamber fuel to increase the pre-chamber pressure which leads to accelerate the injected radicals to leave the pre-chamber volume faster. By measuring the jet travel distance from the nozzle orifice outlet to main chamber, the light emissions appear at distance 14.4 mm for ethanol fuel while it appear at distance 14.21 for gasoline fuel.

Figure 11 shows the in-cylinder pressure traces of both the main and pre-chambers and the corresponding combustion images of lambda 1.2 for ethanol and gasoline. It can clearly notice that the combustion become slower for both fuels. As the main combustion effects the pre-chamber combustion, the pre-chamber combustion become slower and that effects to delay the first appear of the visible chemiluminescence sites in the main chamber to 14 °CA for ethanol and 16 °CA for gasoline. Also, it can notice that the injected jet travel shorter compare to lambda 1.0 where the jet travel distance reduce to 13.85 and 13.23 for ethanol and gasoline, respectively.

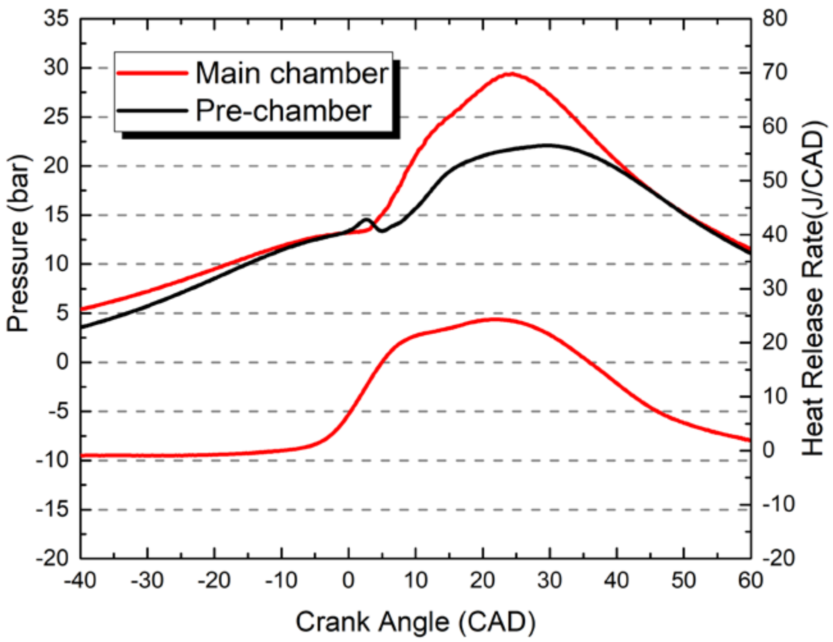

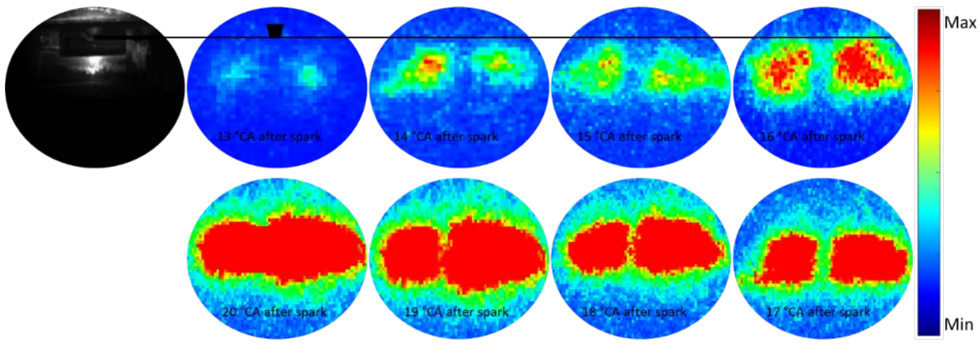

(a) Ethanol Fuel

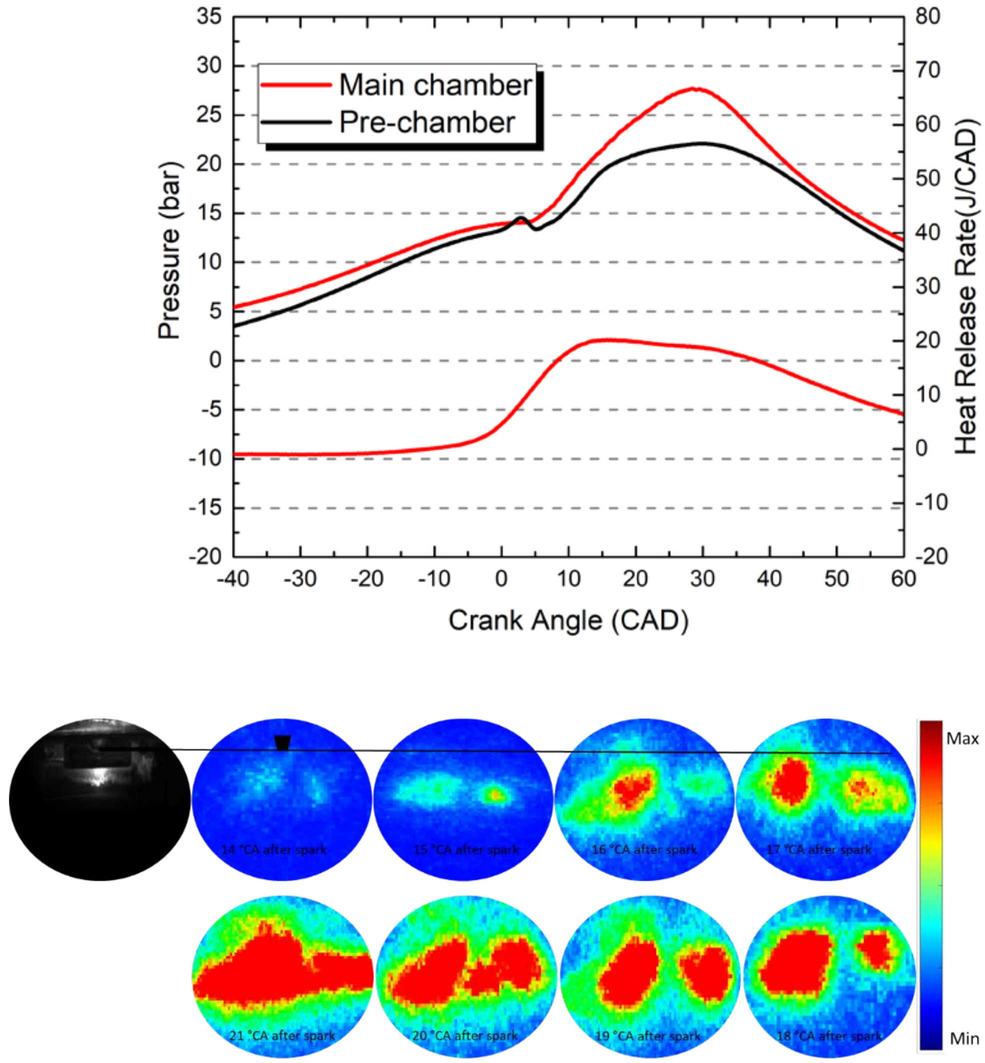

(b) Gasoline Fuel

Figure 10. Pre-chamber and main chamber pressures and ICCD images of ignition sites in the main chamber at fixed spark timing 10 °CA bTDC and λ = 1.0.

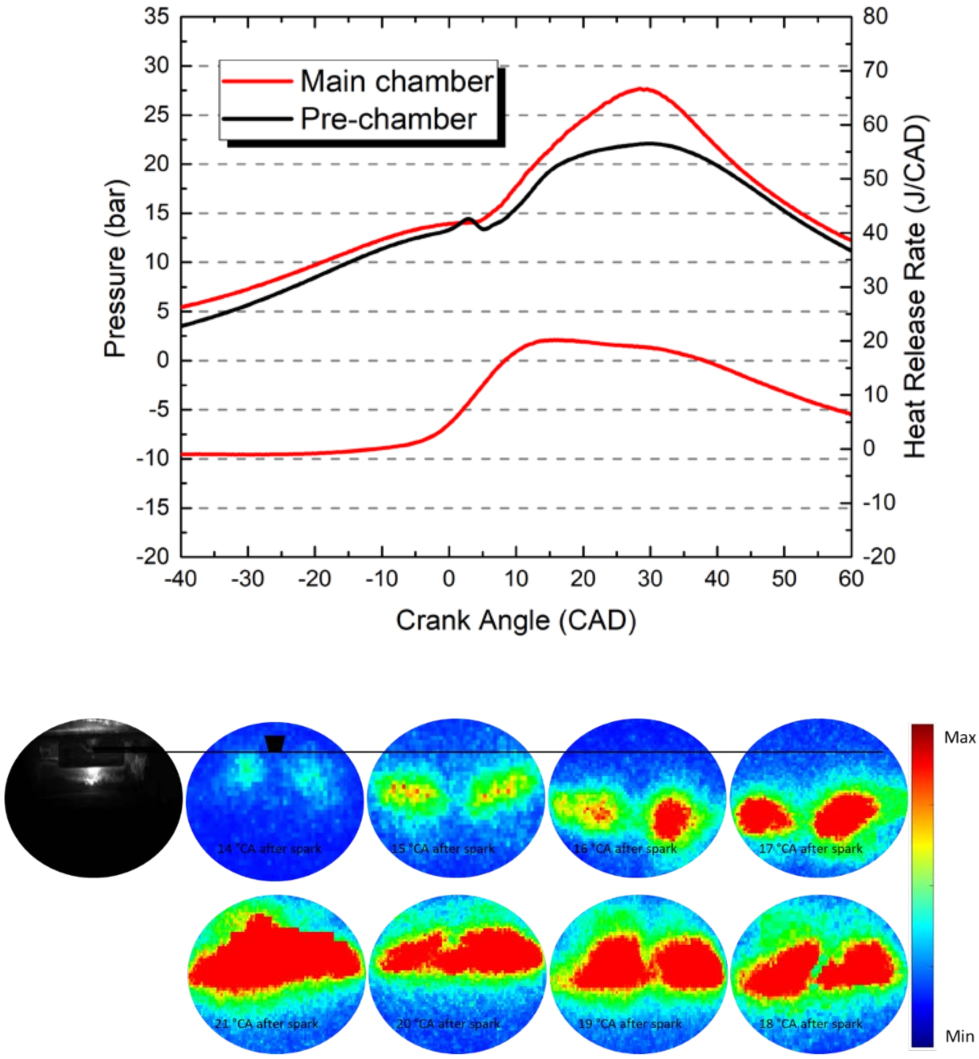

(a) Ethanol Fuel

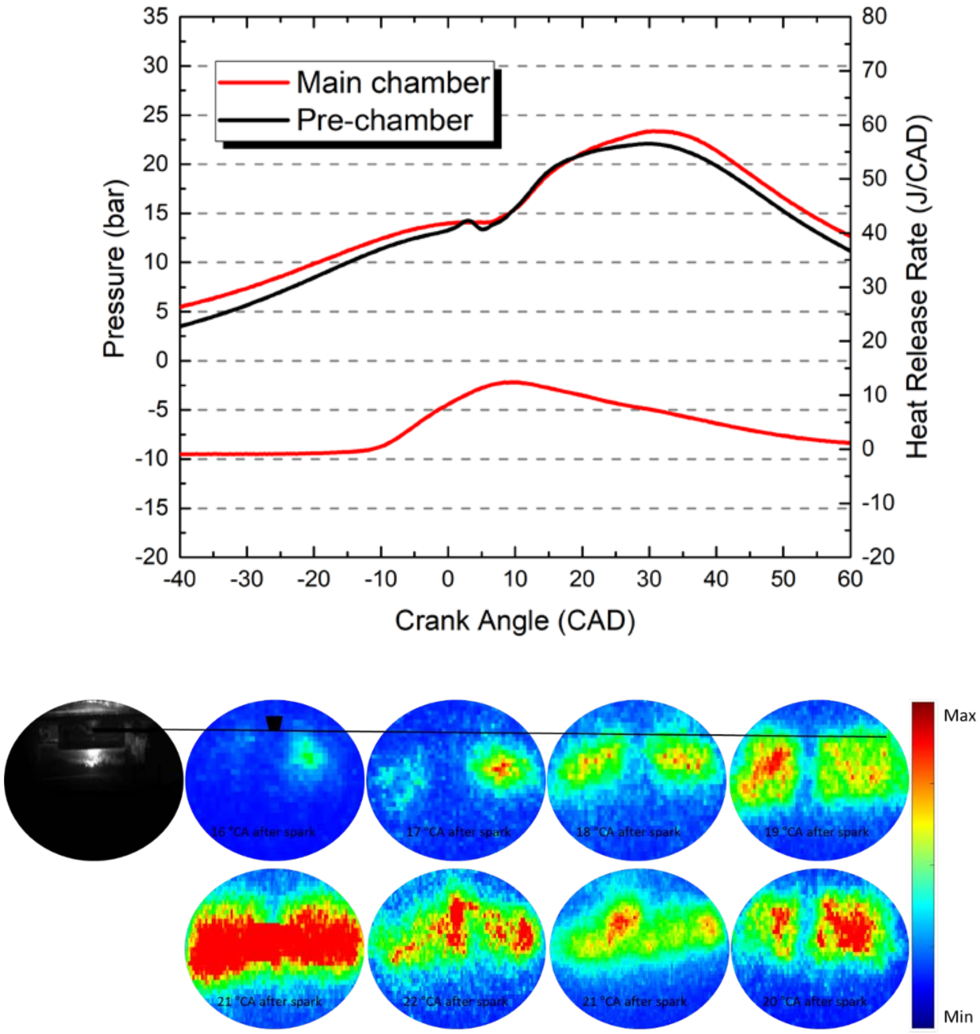

(b) Gasoline Fuel

Figure 11. Pre-chamber and main chamber pressures and ICCD images of ignition sites in the main chamber at fixed spark timing 10 ^{o}CA bTDC and $\lambda = 1.2$.

Next, to reach further lean, fuelled pre-chamber was used. In case of fuelled pre-chamber, the spark timing was fixed at 10 °CA bTDC, start of injection at 50 °CA bTDC and injection fuel 0.3 mg/pulse for both fuels. To have more reliable comparison, lambda of 1.4 was chosen in order to ensure stable, repeatable combustion in the optical engine [12]. The images were obtained for different fuel quantities of 0.3, 0.5 to 0.7 mg/pulse in the pre-chamber. The pre-chamber pressure is acquired by using an AVL GH14D pressure transducer. Figure 12 shows the in-cylinder pressure traces of both the main and pre-chambers and the corresponding combustion images of ethanol. Note that pre-chamber pressure becomes higher than main chamber pressure when spark plug at pre-chamber ignites the air/fuel mixture then combustion continues across the pre-chamber. Because of the increased pre-chamber pressure, the pre-chamber products are injected to main chamber through the nozzle orifices and then captured by the ICCD camera. At fuel injection 0.7 mg/pulse, the visible chemiluminescence sites in the main chamber first appear at 7 ^{o}CA after spark ignition and they are delayed to 9 ^{o}CA, 11 ^{o}CA after spark ignition as the injection duration of ethanol in the pre-chamber was reduced to 0.5 and 0.3 mg/pulse, respectively, which are approximately 2 CAD after pre-chamber pressure rose. The delayed and detached appearance of the light emission sites away from the nozzle clearly demonstrates that these jets were quenched when leaving the orifices. The light emission sites in the first image are coloured in green based on the light intensity and are produced by the hot partially burned jets. The jets first occurs approximately at the point of peak pre-chamber pressure. In the next few frames, the light intensity in the middle region turns into red as the higher temperature combustion occurs and the high temperature region in red expands as the flame fronts continue outward from the jet ignition sites. In addition to their delayed appearance in the main chamber, the location of the first light emission sites become closer to the exit of the pre-chamber when the fuel injected in the pre-chamber is reduced. Measured by the distance from the nozzle orifice outlet, the first light emission sites are reduced from 22.34 to 16.56 and 14.6 mm as the fuel injection in the pre-chamber is reduced from 0.7 mg/pulse, to 0.5 mg/pulse and 0.3 mg/pulse. Also, it is notice that the jet formation size seems decreased. These results can be explained by the greater pressure rise in the pre-chamber which is caused by the more heat released with increasing fuel in the pre-chamber. The larger pressure differential between the pre-chamber and main chamber with more fuel in the pre-chamber results in the jets emanating the nozzle orifices at higher speed and travelled more distance before they are reignited in the main chamber. However, the higher temperature of the jets produced by the burning of more fuel in the pre-chamber reduces the ignition delay of the jets in the main chamber.

For the same reason, similar results are obtained with pre-chamber fuelled with gasoline. The visible jets first appear at 9 ^{o}CA after spark with the fuel injection of 0.7 mg/pulse, and is delayed to 11, 12 ^{o}CA after spark for fuel injection of 0.5 and 0.3 mg/pulse, as shown in figure 13. They are about 2 ^{o}CA later than those of the ethanol operation. The location of the first visible jets are 20.05, 15.51 and 14.31 for fuel injection 0.7, 0.5 and 0.3 mg/pulse, respectively. They are slightly shorter than those of the ethanol, because the pre-chamber pressure is lower than that of ethanol by 2 bar.

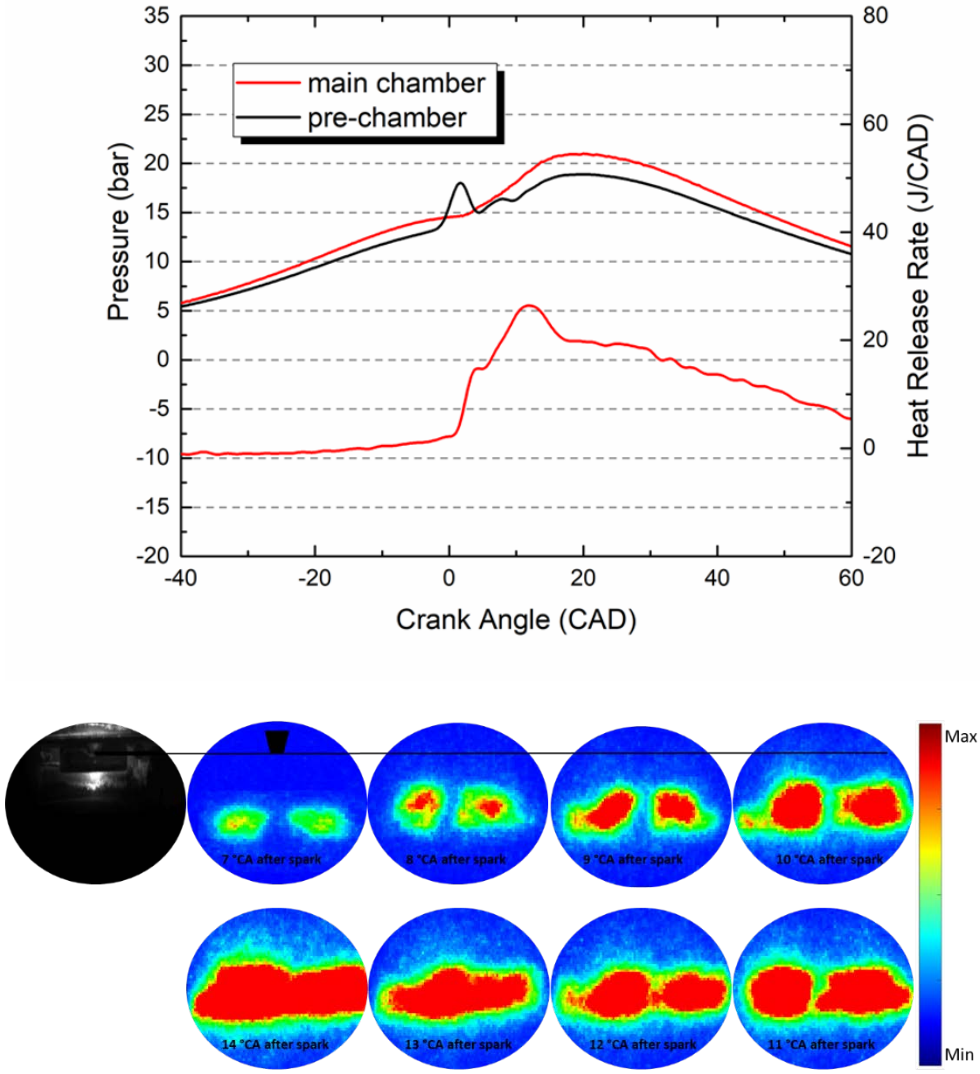

(a) fuel injection 0.7 mg/pulse

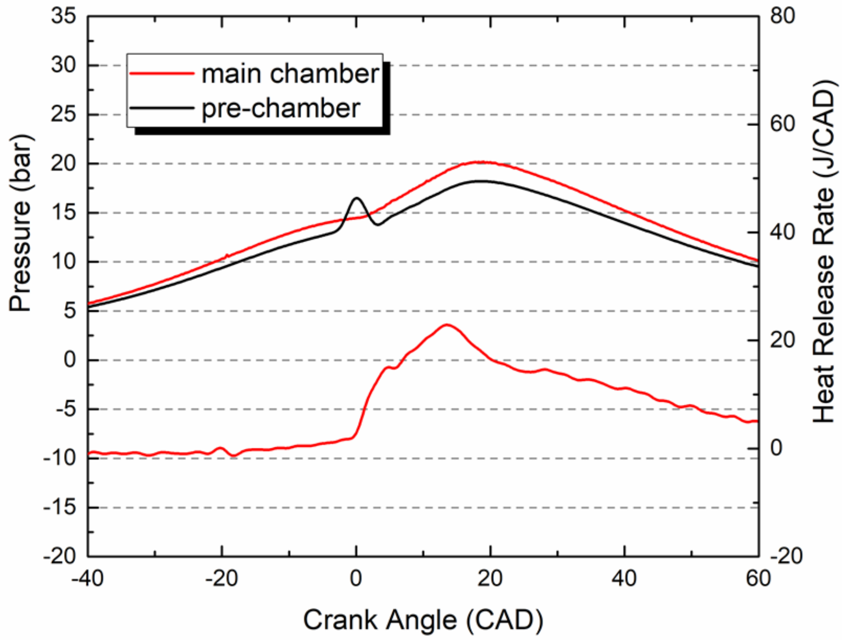

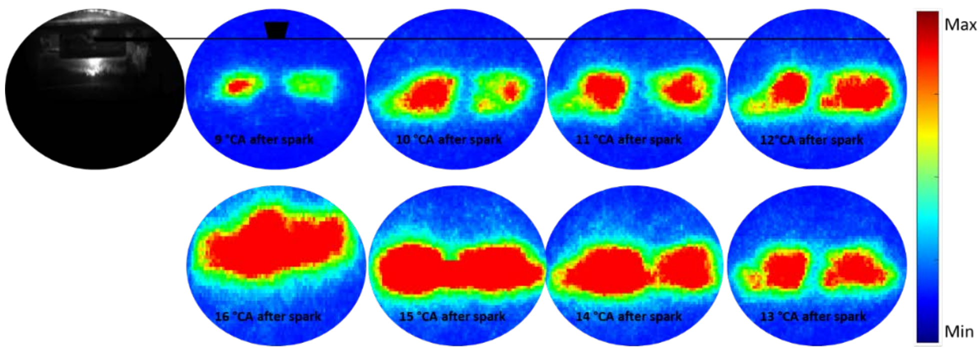

(b) fuel injection 0.5 mg/pulse

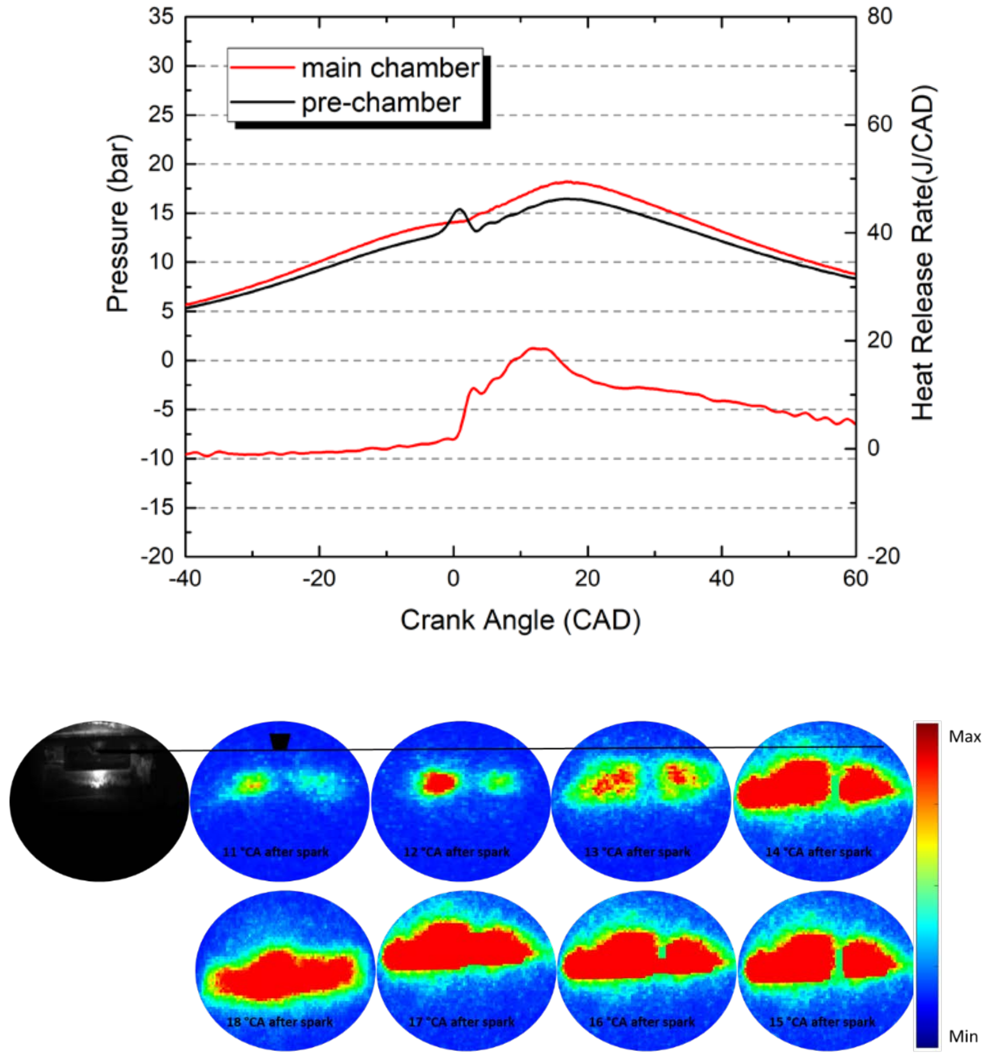

(c) fuel injection 0.3 mg/pulse

Figure 12. Pre-chamber and main chamber pressure and ICCD images of ignition sites in the main chamber at fixed injection timing 50 °CA bTDC and spark timing 10 °CA bTDC fuelled by ethanol under fuel injection duration is 0.3, 0.5 and 0.7 mg/pulse.

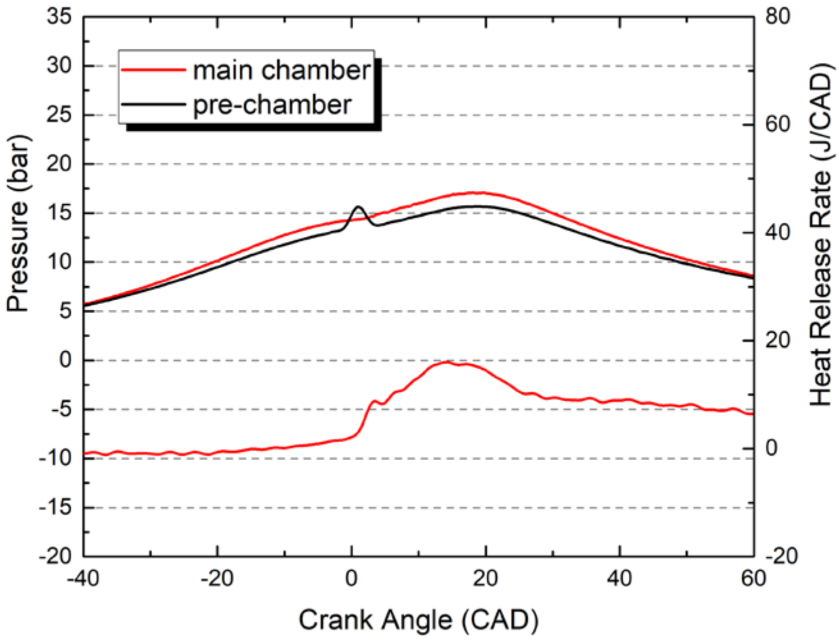

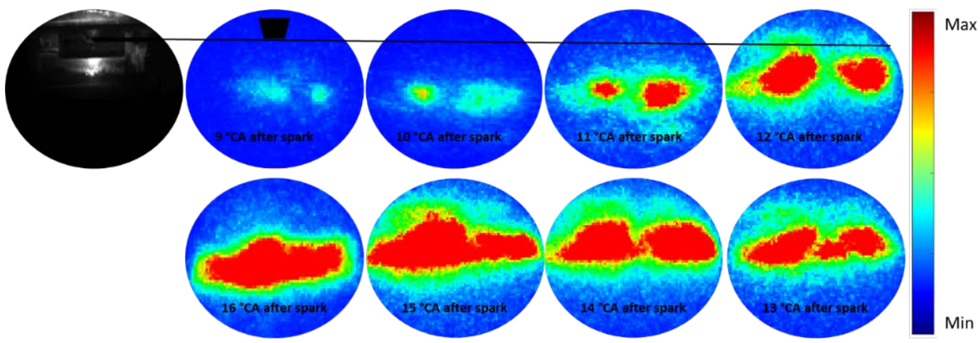

(a) fuel injection 0.7 mg/pulse

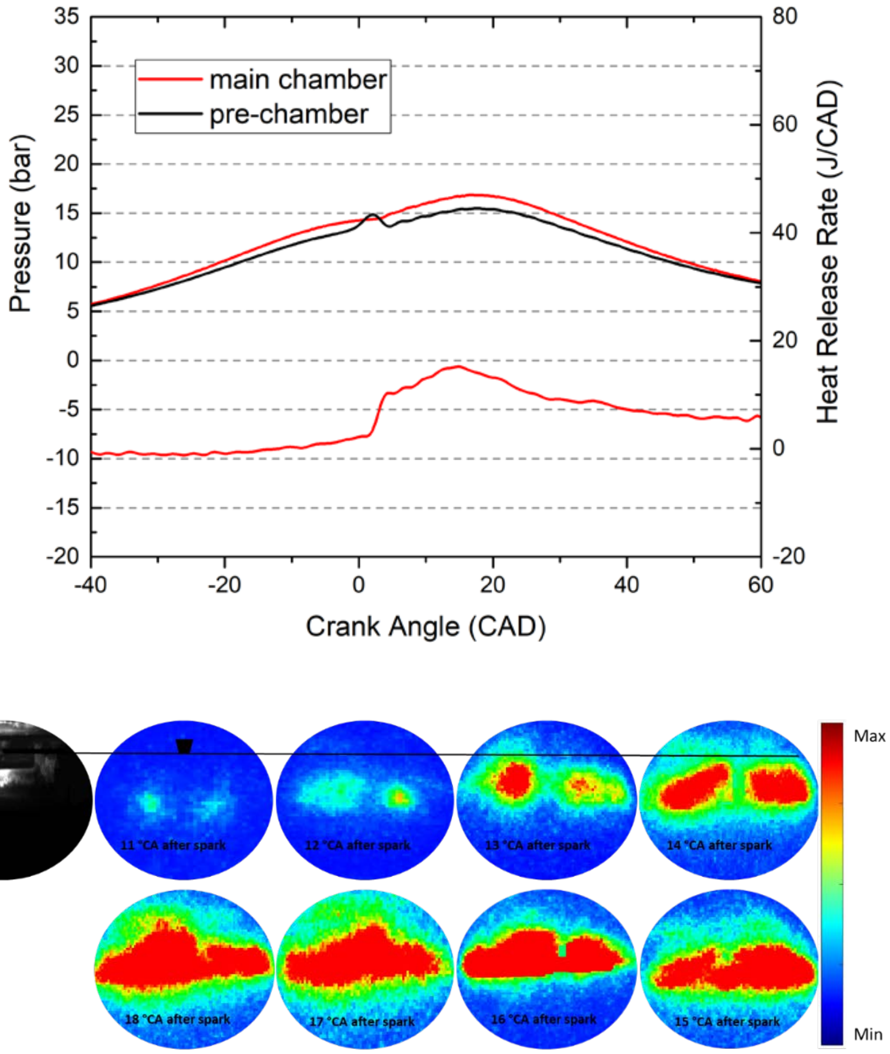

(b) fuel injection 0.5 mg/pulse

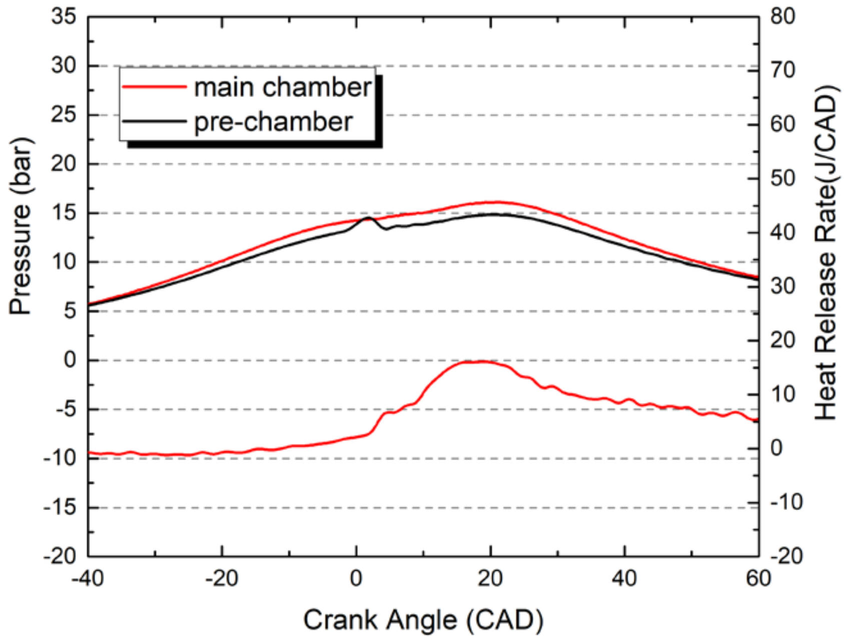

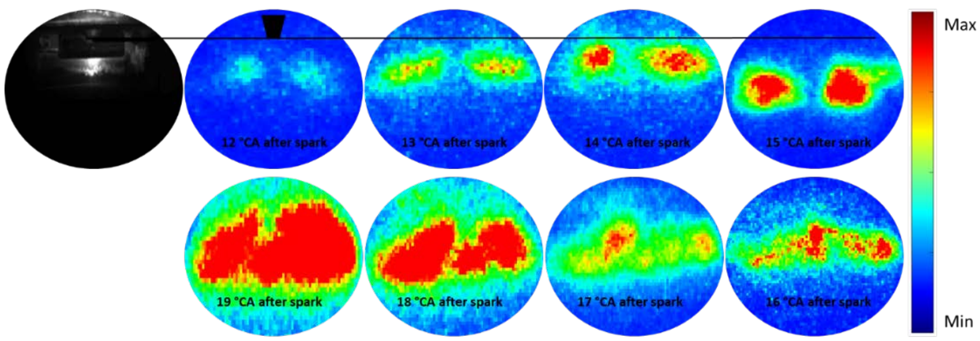

(c) fuel injection 0.3 mg/pulse

Figure 13. Pre-chamber and main chamber pressures and ICCD images of ignition sites in the main chamber at fixed injection timing 50 °CA bTDC and spark timing 10 °CA bTDC fuelled by gasoline under fuel injection duration is 0.3, 0.5 and 0.7 mg/pulse.

Figure 14 shows the jet travel distance and injection delay for both fuel at fixed injection timing 50 °CA bTDC and spark timing 10 °CA bTDC under different fuel injection duration is 0.3, 0.5 and 0.7 mg/pulse. The figure illustrates the effect of fuel type and fuel injection at injected pre-chamber products. Ethanol fuel at different fuel injection duration shows that it has great effect on injected products compare to gasoline. Moreover, at fuel injection duration 0.7 mg/pulse the injected radicals travel deeper and the jet flame appear faster.

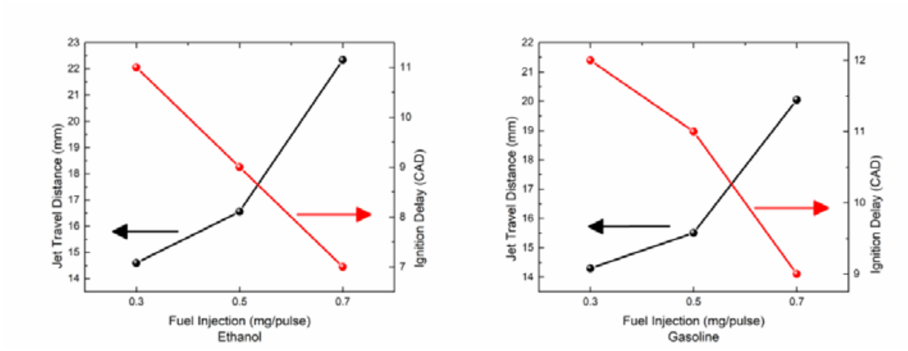

Figure 14. Shows the jet travel distance and ignition delay for both fuel at different fuel injections 0.3, 0.5 and 0.7 mg/pulse.

Additionally, the effect of injection timing and spark timing in the pre-chamber are studied. The fuel injection was fixed at 0.3 mg/pulse, spark timing at 10 °CA bTDC while the start of pre-chamber injection was changed to 30, 50 and 70 °CA bTDC. The results show that the injection timing has less effect on combustion stability as shown in figure 15. However, as the injection timing was advanced to 70 °CA bTDC, the combustion became unstable. Based on the combustion stability, the start of injection at 50 °CA bTDC is an optimal for both fuels. The results indicate that the actual mixture strength at the time of the pre-chamber spark ignition varied with the pre-chamber injection, which could be caused by the interaction of the air flow into the pre-chamber. Fuel injected too early in the pre-chamber was likely to become more diluted at the time of spark ignition by the incoming air. Whereas very late injection in the pre-chamber may not be able to produce a near stoichiometric mixture at the point of spark discharge. Finally, the effect of spark timing in the fuelled pre-chamber was investigated by fixing the injection at 50 °CA bTDC, fuel injection 0.3 mg/pulse for both fuels as shown in figure 15. It was noticed that as the spark timing advanced the combustion become unstable. However, ethanol shows more combustion stability under all spark timing compared to gasoline. This is because ethanol had the fastest flame speed and ethanol appeared to exhibit less cyclic variation.

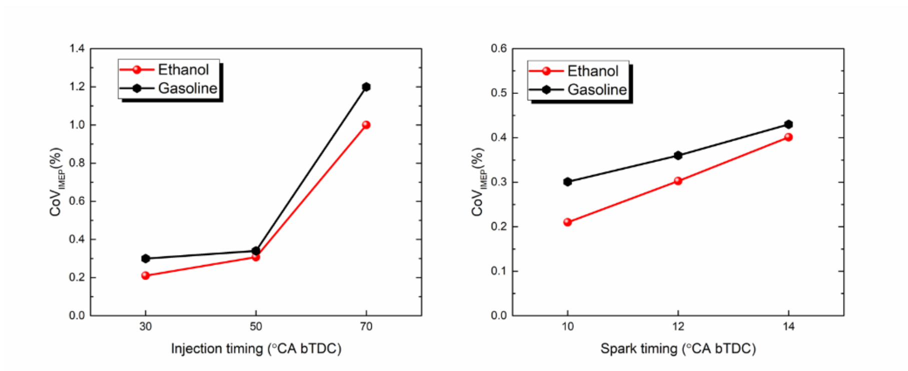

Figure 15. The effect of pre-chamber fuel injection timing and spark timing for ethanol and gasoline.

6. Conclusions

In this study, effects of pre-chamber ignition with or without gasoline or ethanol were investigated by means of in-cylinder pressure and high speed optical at a constant engine speed of 1200 rpm and wide open throttle. High speed and ICCD cameras were used to capture the ignition and combustion processes in the combustion chamber.

The results show that, at the fixed spark timing of 10 °CA bTDC and injection at 50 °CA bTDC in the pre-chamber, increasing the fuel injected in the pre-chamber from 0.3, to 0.5 and 0.7 mg/pulse, the pre-chamber pressure rises faster to a higher peak value, producing greater pressure differential between the pre and main chamber and faster turbulent jets of partially burned products at higher temperature. The increasing in the pre-chamber pressure causes the jets to travel deeper into the main chamber and the ignition sites become bigger, though the ignition delay of the main chamber combustion becomes shorter as the temperature of jets is higher. The turbulent ignition jets of ethanol are characterised with greater momentum than gasoline due to the faster combustion speed of ethanol and higher energy input. In comparison, the pre-chamber fuel injection timing has less effect. However, it was noticed that at injection timing of 70 °CA bTDC the combustion becomes unstable. It was noticed that as the spark timing advanced the combustion become unstable.

References

1- Wu, X., Daniel, R., Tian, G., Xu, H., Huang, Z., & Richardson, D. (2011). Dual-injection: The flexible, bi-fuel concept for spark-ignition engines fuelled with various gasoline and biofuel blends. Applied Energy, 88(7), 2305-2314.
2- El-Faroug, M. O., Yan, F., Luo, M., & Fiifi Turkson, R. (2016). Spark Ignition Engine Combustion, Performance and Emission Products from Hydrous Ethanol and Its Blends with Gasoline. Energies, 9(12), 984.
3- R. A. Stein, J. E. Anderson, and T. J. Wallington, "An Overview of the Effects of Ethanol-Gasoline Blends on SI Engine Performance, Fuel Efficiency, and Emissions," SAE Int. J. Engines, vol. 6, no. 1, pp. 2013-01–1635, Apr. 2013.
4- US Ethanol Industry: the next inflection point. BCurtis Energies and Resource Group, 2007 year in review; 2008.
5- Goldemberg J. The challenge of biofuels. Energy Environ Sci 2008;1:523–5
6- Toulson, E., Schock, H., and Attard, W., "A Review of Pre-Chamber Initiated Jet Ignition Combustion Systems," SAE Technical Paper 2010-01-2263, 2010, https://doi.org/10.4271/2010-01-2263.
7- Dale, J. D., Checkel, M. D. and Smy, P. R., "Application of High Energy Ignition Systems to Engines", Progress in Energy and Combustion Science, 1997. 23 (5-6), 379-398.
8- Chinnathambi, P., Bunce, M., and Cruff, L., "RANS Based Multidimensional Modeling of an Ultra-Lean Burn Pre-Chamber Combustion System with Auxiliary Liquid Gasoline Injection," SAE Technical Paper 2015-01-0386, 2015, doi:10.4271/2015-01-0386.
9- Attard, W. and Blaxill, H., "A Lean Burn Gasoline Fueled Pre-Chamber Jet Ignition Combustion System Achieving High Efficiency and Low NOx at Part Load," SAE Technical Paper 2012-01-1146, 2012, https://doi.org/10.4271/2012-01-1146.
10- Bunce, M. and Blaxill, H., "Methodology for Combustion Analysis of a Spark Ignition Engine Incorporating aPre-Chamber Combustor," SAE Technical Paper 2014-01-2603, 2014, doi:10.4271/2014-01-2603.
11- Heywood, J.B., Automotive Engines and Fuels: A Review of Future Options. Progress in Energy and Combustion Science, Vol. 7, Iss. 3., pp.155-184, 1981.
12- Bunce, M., Blaxill, H., Kulatilaka, W., and Jiang, N., "The Effects of Turbulent Jet Characteristics on Engine Performance Using a Pre-Chamber Combustor," SAE Technical Paper 2014-01-1195, 2014, doi:10.4271/2014-01-1195.
13- Turkish, M.C., "3-Valve Stratified Charge Engines: Evolvement, Analysis and Progression," SAE Technical Paper 741163, 1974, doi:10.4271/741163.

14- Noguchi, N., Sanda, S. and Nakamura, N., “Development of Toyota Lean Burn Engine,” SAE Technical Paper 760757, 1976, doi:10.4271/760757.
15- Gussak, L.A., Karpov, V.P. and Tikhonov, Y.Y., “The Application of the Lag-Process in Pre-chamber Engines,” SAE Technical Paper 790692, 1979, doi:10.4271/790692.
16- Maxson, J.A., Hensinger, D.M., Horn, K., and Oppenheim, A.K., “Performance of Multiple Stream Pulsed Jet Combustion Systems,” SAE Technical Paper 910565, 1991, doi:10.4271/910565.
17- Latsch, R., “The Swirl Chamber Spark Plug: A Means of Faster, More Uniform Energy Conversion in the Spark Ignition Engine,” SAE Technical Paper 840455, 1984, doi: 10.4271/840455.
18- Toulson, E., Watson, H.C., and Attard, W.P., “Gas Assisted Jet Ignition of Ultra-Lean LPG in a Spark Ignition Engine,” SAE Technical Paper 2009-01-0506, 2009, doi: 10.4271/2009-01-0506.
19- Lezanski, T., Kesler, M., Rychter, T., Teodorczyk, A., and Wolanski, P., “Performance of a Pulsed Jet Combustion (PJC) System in a Research Engine,” SAE Technical Paper 932709, 1993, doi:10.4271/932709.
20- Kito, S., Wakai, K., Takahashi, S., Fukaya, N., and Takada, Y., Ignition Limit of Lean Mixture by Hydrogen Flame Jet Ignition. JSAE Review, 2000. 21(3): 373-378.
21- Couet, S., Higelin, P., and Moreau, B., “APIR: A New Firing Concept for the Internal Combustion Engines -Sensitivity to Knock and In-Cylinder Aerodynamics,” SAE Technical Paper 2001-01-1954, 2001, doi: 10.4271/2001-01-1954.
22- Kettner, M., Rothe, M., Velji, A., Spicher, U., Kuhnert, D., and Latsch, R., “A New Flame Jet Concept to Improve the Inflammation of Lean Burn Mixtures in SI Engines” SAE Technical Paper 2005-01-3688, 2005, doi:10.4271/2005-01-3688.
23- Najt, P.M., Rask, R.B., and Reuss, D.L., Dual Mode Engine Combustion Process. 2003: United States Patent No.6595181.
24- Kojic, A., Hathout, J.-P., Cook, D., and Ahmed, J., Control of Auto-Ignition Timing for Combustion in Piston Engines by Prechamber Compression Ignition. 2005: United States Patent No. PCT/US2004/029612.
25- Pape, J., Getzlaff, J., Gruenig, C., Kuhnert, D., and Latsch, R., “Investigations on Pre-Chamber Spark Plug with Pilot Injection,” SAE Technical Paper 2007-01-0479, 2007, doi:10.4271/2007-01-0479.
26- Regueiro, J., "The Case for New Divided-Chamber Diesel Combustion SystemsPart Two: Critical Analysis of, and Solutions for, Swirl-Prechamber Engines," SAE Technical Paper 2001-01-0274, 2001, https://doi.org/10.4271/2001-01-0274.
27- Toulson, E., Watson, H., and Attard, W., "Gas Assisted Jet Ignition of Ultra-Lean LPG in a Spark Ignition Engine," SAE Technical Paper 2009-01-0506, 2009, https://doi.org/10.4271/2009-01-0506.
28- Toulson, E., Schock, H., and Attard, W., "A Review of Pre-Chamber Initiated Jet Ignition Combustion Systems," SAE Technical Paper 2010-01-2263, 2010, https://doi.org/10.4271/2010-01-2263.
29- Russ, Stephen. A review of the effect of engine operating conditions on borderline knock. No. 960497. SAE Technical Paper, 1996.